CHAPTER V

SOLUTION PROCEDURE OF SECURITY CONSTRAINED OPTIMAL POWER FLOW

5.1 Introduction

The formulation of security constrained optimal power flow (SCOPF) problem is presented in this chapter. Then, the sequential and the parallel of SADE_ALM for solving the SCOPF problems are presented, followed by numerical test results. The conclusion is provided in the last section.

5.2 Security Constrained Optimal Power Flow (SCOPF) Problem Formulation

The security constrained optimal power flow (SCOPF) problem is to optimize the total generator fuel cost function subject to power balance constraints and inequality constraints of the base-case state as well as the contingency-case states. Mathematically, the SCOPF problem can be formulated as follows:

$$Min\ J(X,U) \tag{5.1}$$

subject to

1) equality and inequality constraints of the base-case state

$$h(X,U)=0 \tag{5.2}$$

$$g(X,U)\le 0 \tag{5.3}$$

2) equality and inequality constraints of the contingency-case states

$$h^R(X,U^R)=0,\ R=1,...,NO \tag{5.4}$$

$$g^R(X,U^R)\le 0,\ R=1,...,NO \tag{5.5}$$

where

U and U^R are the vectors of state variables of the base-case and the contingency-case states respectively, consisting of real power of slack generator P_{G_1}, voltage magnitude of load bus V_L, reactive power of all generators Q_G, transformer and transmission line loadings S_l. Therefore, U (or U^R) can be expressed as $U(or\ U^R)=[P_{G_i},V_{L_1},...,V_{L_{NL}},Q_{G_1},...,Q_{G_{NG}},S_{l_1},...,S_{l_{NBR}}]^T$ where NL, NG, NBR, and NO are number of load buses, number of generators, number of transformers and

transmission lines, and numbers of contingency constraints to be considered, e.g. *N*-1 transmission line outages respectively.

X is the vector of control variables consisting of real power of all generators excluding slack generator, voltage magnitude of all generators V_G, and transformer tap settings T. Therefore, X can be expressed as $X = [P_{G_2},...,P_{G_{NG}},V_{G_1},...,V_{G_{NG}},T_1,...,T_{NT}]^T$ where NT is the number of regulating transformers.

$h(X,U)$ and $h^R(X,U^R)$ are the equality constraints of the base-case and the contingency-case states respectively, representing typical power flow equations.

$g(X,U)$ and $g^R(X,U^R)$ are the inequality constraints of the base-case and the contingency-case states respectively, representing system operating constraints.

$J(X,U)$ is the objective function to be minimized. Generally, in the SCOPF problem, the objective function J is the total generator fuel cost, i.e.

$$J = \sum_{i=1}^{NG} f_i\left(P_{G_i}\right) \tag{5.6}$$

where $f_i(\cdot)$ is the fuel cost function of the ith generator.

The fuel cost function is typically represented by simple quadratic function as in (5.7).

$$f_i\left(P_{G_i}\right) = a_i P_{G_i}^2 + b_i P_{G_i} + c_i \tag{5.7}$$

where P_{G_i} is the real power of the ith generator, and a_i, b_i, and c_i are the fuel cost coefficients.

The system operating constraints of both base-case state and contingency-case states can be described below.

1) Generation constraints: Real and reactive power outputs, and voltage magnitude of generators are restricted by the lower and upper limits, i.e.

$$V_{G_i}^{min} \le V_{G_i} \le V_{G_i}^{max}, \quad i \in NG \tag{5.8}$$

$$P_{G_i}^{min} \le P_{G_i} \le P_{G_i}^{max}, \quad i \in NG \tag{5.9}$$

$$Q_{G_i}^{min} \le Q_{G_i} \le Q_{G_i}^{max}, \quad i \in NG \tag{5.10}$$

2) Transformer constraints: Transformer tap settings are restricted by the lower and upper limits as follows:

$$T_i^{min} \le T_i \le T_i^{max}, \qquad i \in NT \tag{5.11}$$

3) Security constraints: These include the constraints of voltage magnitude at load buses and power flow through transformers and transmission line (MVA loading) as follows:

$$V_{L_i}^{min} \le V_{L_i} \le V_{L_i}^{max}, \qquad i \in NL \tag{5.12}$$

$$S_{l_i} \le S_{l_i}^{max}, \qquad i \in NBR \tag{5.13}$$

As in chapter 4, the inequality constraints of the state variables of the base-case and the contingency-case states are handled using the augmented lagrange multiplier (ALM) method to avoid ill-conditioning of the traditional penalty function method as show below [1, 2].

$$\begin{aligned} L_a = {} & f(X,U) + \\ & r_g\left[\sum_{j=1}^{m}\left\{max\left[g_j(X,U), -\frac{\beta_j}{2r_g}\right]\right\}^2 + \sum_{R=1}^{NO}\sum_{j=1}^{m}\left\{max\left[g_j^R(X,U^R), -\frac{\beta_j}{2r_g}\right]\right\}^2\right] + \\ & \sum_{j=1}^{m}\beta_j\left[\left\{max\left[g_j(X,U), -\frac{\beta_j}{2r_g}\right]\right\} + \sum_{R=1}^{NO}\sum_{j=1}^{m}\left\{max\left[g_j^R(X,U^R), -\frac{\beta_j}{2r_g}\right]\right\}\right] \end{aligned} \tag{5.14}$$

where

$g_j(\cdot)$, j = 1,2,..., m, m = 2*(1+NL+NG)+NBR are the m-inequality constraints of the state variables of the base-case state,

$g_j^R(\cdot)$,R=1,...,NO, j = 1,2,..., m, m = 2*(1+NL+NG)+NBR are the m-inequality constraints of the state variables of the contingency-case states,

r_g is the positive penalty multiplier, and

β_js are the lagrange multipliers of the inequality constraints of the base-case and the contingency-case states.

The inequality constraints of base-case state and contingency-case states can be defined as follows:

1) real power of slack generator,

$$g_1 = \left(-P_{G_1} + P_{G_1}^{\min}\right) \tag{5.15}$$

$$g_2 = \left(P_{G_1} - P_{G_1}^{\max}\right) \tag{5.16}$$

2) voltage magnitude of load buses V_{L_i}, $i = 1,\ldots, NL$

$$g_i = \left(-V_{L_i} + V_{L_i}^{\min}\right) \tag{5.18}$$

$$g_{i+1} = \left(V_{L_i} - V_{L_i}^{\max}\right) \tag{5.19}$$

3) reactive power of generators Q_{G_i}, $i = 1,\ldots, NG$

$$g_i = \left(-Q_{G_i} + Q_{G_i}^{\min}\right) \tag{5.20}$$

$$g_{i+1} = \left(Q_{G_i} - Q_{G_i}^{\max}\right) \tag{5.21}$$

4) transformer and transmission line loadings S_{l_i}, $i = 1,\ldots, NBR$

$$g_i = \left(S_{l_i} - S_{l_i}^{\max}\right) \tag{5.22}$$

After the unconstrained minimization problem has been solved, the lagrange multipliers and the penalty parameter will be updated to create the new augmented lagrange function L_a as follows [1, 2]:

$$\beta_j^{i+1} = \beta_j^i + 2r_g\left[\left\{max\left[g_j(X,U), -\frac{\beta_j^i}{2r_g}\right]\right\} + \sum_{R=1}^{NO}\left\{max\left[g_j^R\left(X,U^R\right), -\frac{\beta_j^i}{2r_g}\right]\right\}\right] \tag{5.23}$$

$$r_g^{i+1} = \begin{cases} c_g \times r_g^i, & if\ r_g^i \le r_{g,max} \\ r_{g,max}, & otherwise \end{cases} \tag{5.24}$$

where c_g is the positive constant increasing rate, and $r_{g,max}$ is the maximum penalty multiplier.

The lagrange multipliers β_js in (5.23) are deterministically updated using the inequality constraint functions evaluated from the previous solution of the unconstrained minimization problem, while the penalty parameter r_g is increased by a constant rate until it reaches the predetermined maximum value as shown in (5.24). The algorithm is then repeated until termination. The detail of the proposed algorithms will be described in the next section.

5.3 SADE_ALM based security constrained optimal power flow (SADE_ALM-SCOPF)

As in section 4.3 of chapter 4, the proposed self-adaptive differential evolution with augmented lagrange multiplier method (SADE_ALM) consists of two iterative loops, i.e. the inner loop and the outer loop. The inner loop solves the unconstrained minimization problem through the augmented lagrange function L_a using self-adaptive differential evolution (SADE).

After the unconstrained minimization problem has been solved, the outer loop will update the lagrange multipliers βs and the penalty parameter r_g by the ALM method, to create the new augmented lagrange function L_a. The algorithm is then repeated until a termination criterion, i.e. 1) maximum number of iterations, or 2) convergence of the optimal solution, is reached. The flowchart of the SADE_ALM when applied to solve the SCOPF problems is shown in Figure 5.1.

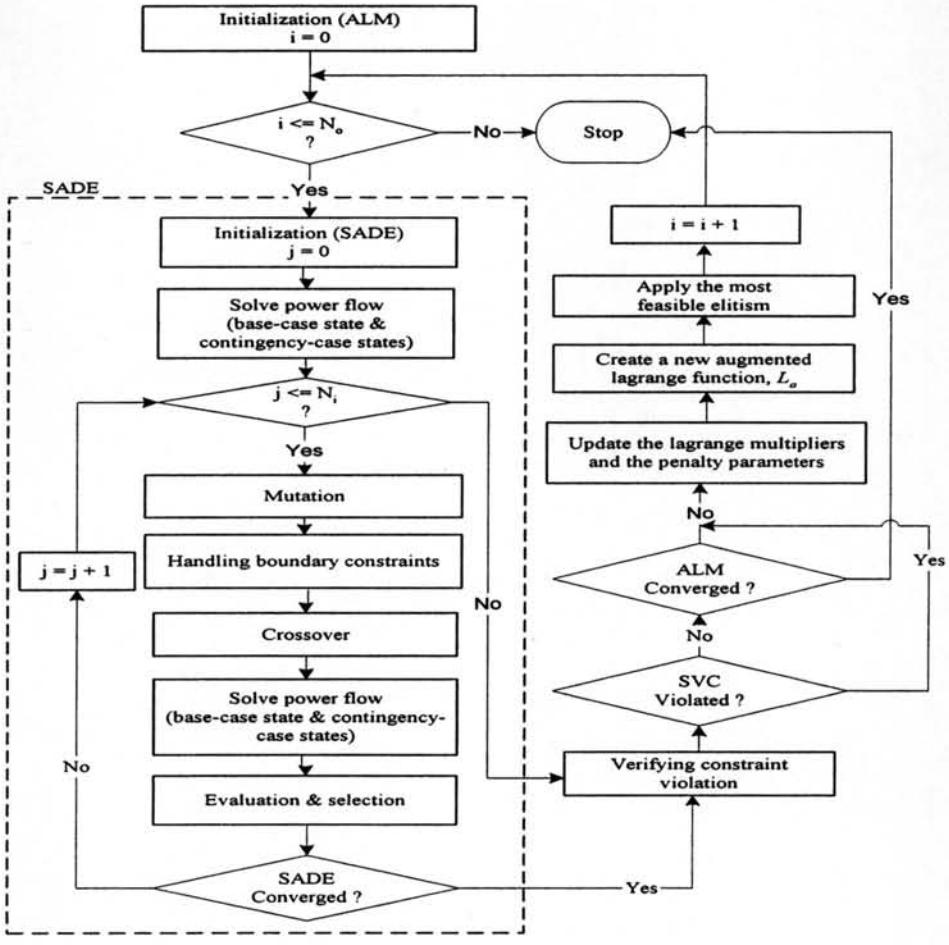

Figure 5.1 Flowchart of SADE_ALM-SCOPF

5.3.1 The inner loop iteration

The inner loop solves the augmented lagrange function L_a using self-adaptive differential evolution (SADE). The algorithm of the inner loop iteration is the same as in section 4.3.1 of chapter 4. However, it is important to note that power flow solutions in step 2) of the inner loop iteration have to calculate both the base case and contingency case states to determine all the state variables of the associated individual X_j. If the power flow of any individual fails to converge,

such individual will be removed and replaced by new randomly generated individuals. This process is repeated until the power flow calculations of such individuals are converged. In addition, in the evaluation and selection of step 6), the fitness value (i.e., the augmented objective value) of the trial vector $X_j^{\prime\prime(G)}$ is compared with its parent vector $X_j^{(G)}$ using (5.14) instead of (4.15).

5.3.2 The outer loop iteration

After the inner loop has converged, the outer loop is started by using the ALM method to handle the inequality constraints of the state variables. The details of the outer loop iteration are described as in the following.

1) Initialization

Set maximum iteration of the outer loop (N_o), the constrain violation tolerance (ε_{SVC}), the lagrange multiplier βs, and the penalty parameters r_g including c_g, and $r_{g,max}$.

2) Verifying constrain violation

The constrain violation of the optimal solution obtained from the inner loop (X_{opt}^{*}) is verified through the sum of the violated constraints (SVC) index as shown in (5.25) and (5.26).

$$SVC \le \varepsilon_{SVC} \tag{5.25}$$

$$SVC = \sum_{j=1}^{m} \left\{ max\left[g_j\left(X_{opt}^{*}\right), 0 \right] \right\} + \sum_{R=1}^{NO} \sum_{j=1}^{m} \left\{ max\left[g_j^{R}\left(X_{opt}^{*}\right), 0 \right] \right\} \tag{5.26}$$

where $g_j(\cdot)$, and $g_j^R(\cdot)$,$R=1,...,NO$, j = 1,2,..., m , m = 2*(1+NL+NG)+NBR are the m-inequality constraints of the state variables of the base-case and the contingency-case states respectively as explained in section 5.2.

3) Creating a new unconstrained minimization problem

To create a new unconstrained minimization problem for the next inner loop iteration, the new augmented lagrange function L_a is created by updating the lagrange multiplier βs and the penalty parameter r_g according to (5.23), and (5.24) respectively.

4) Appling the most feasible elitism

To improve the efficiency of the proposed algorithm, the most feasible elitism (X_{elite}) is employed by replacing the worst individual X_j which has the highest fitness value for the next inner loop iteration. The elitist member is initialized by using the optimal solution obtained from

the first outer loop iteration. Then, it is updated according to the extent of the violated *SVC* value and the total generator fuel cost in (5.6) as described in section 4.3.2 of chapter 4. The outer loop will be terminated according to the same two criteria as defined for the inner loop, i.e. 1) maximum iteration number of the outer loop (N_o), and 2) convergence of the optimal solution.

5.4 Parallel SADE_ALM Based Security Constrained Optimal Power Flow (pSADE_ALM-SCOPF)

As in section 4.4 of chapter 4, the proposed pSADE_ALM is a modified version of sequential self-adaptive differential evolution (SADE_ALM) [1, 2] by exploiting parallel processing techniques to increase the search capability of the algorithm via PC cluster 3x2.8 GHz Pentium IV processors arranged in master-slave structure with 256 MB RAM for each PC.

The proposed pSADE_ALM consists of two iterative loops, i.e. the inner loop, and the outer loop. The inner loop iteration is implemented independently by all PCs with three DE's strategies, i.e. DE/rand/1/bin, DE/rand-to-best/1/bin, and DE/best/2/bin are assigned to slave node 1, slave node2, and master node respectively. For each PC, the inner loop iteration solves the unconstrained minimization problem through the augmented lagrange function L_a using self-adaptive differential evolution (SADE). After the unconstrained minimization problem has been solved independently by all PCs, the master node will implement the outer loop iteration. Firstly, the master node will compare and determine the best optimal result from all PCs based on the extent of the constraint violation and the total generator fuel cost. Then, the master node will update the lagrange multipliers βs and the penalty parameter r_g to create the new augmented lagrange function $L_{a'}$. The algorithm is then repeated until a termination criterion, i.e. maximum number of iterations or convergence of the optimal solution, is reached. The flowchart of the pSADE_ALM when applied to solve the SCOPF problems is shown in Figure 5.2.

5.4.1 The inner loop iteration

For each PC, the inner loop solves the augmented lagrange function L_a using self-adaptive differential evolution (SADE) based on its DE's strategy. The algorithm of the inner loop iteration is described in section 4.4.3 of chapter 4. However, power flow solutions in step 2) of the inner loop iteration of each PC have to calculate both the base case and contingency case states to determine all the state variables of the associated individual X_j. If the power flow of any

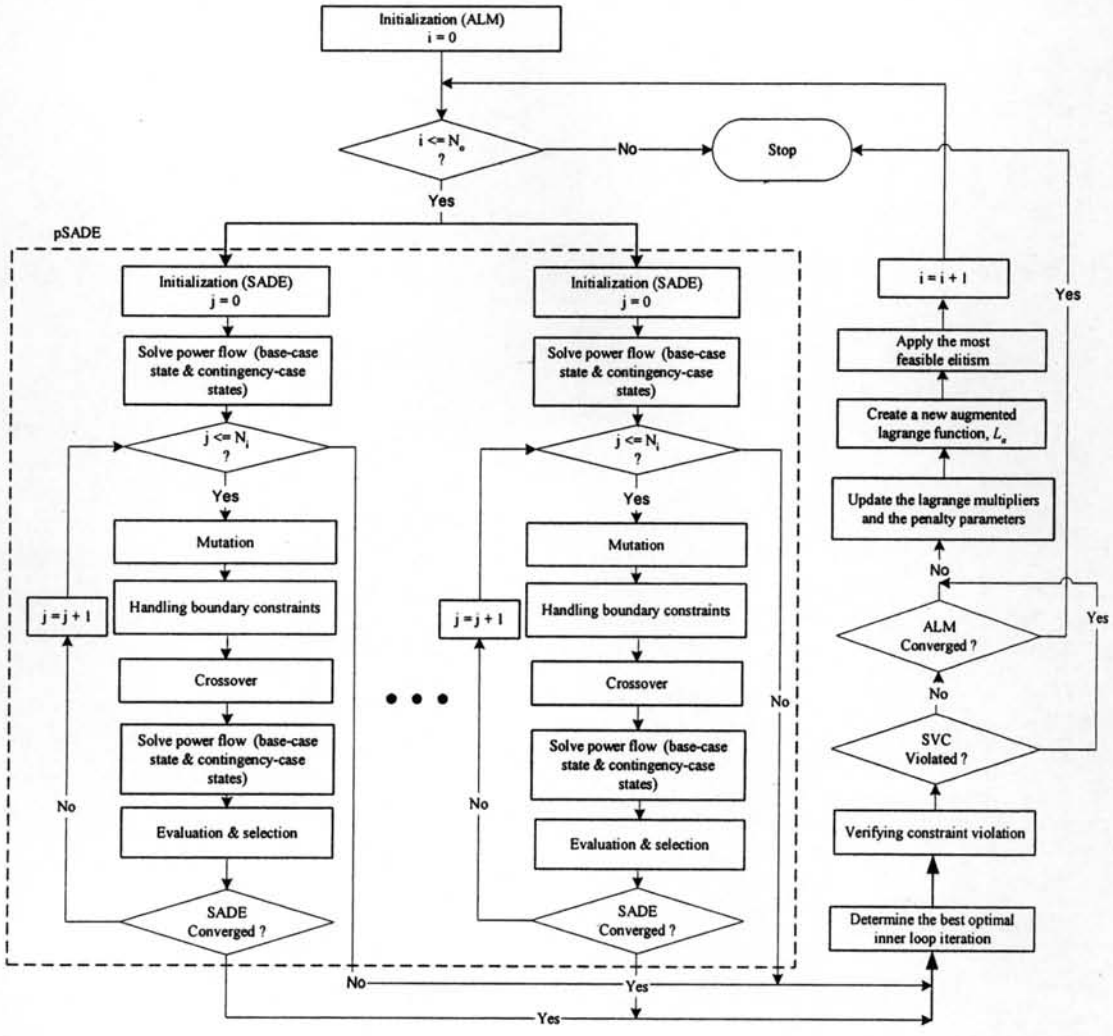

Figure 5.2 Flowchart of pSADE_ALM-SCOPF

individual fails to converge, such individual will be removed and replaced by new randomly generated individuals. This process is repeated until the power flow calculations of such individuals are converged. In addition, in the evaluation and selection of step 6), the fitness value (i.e., the augmented objective value) of the trial vector $X_j^{\prime\prime(G)}$ is compared with its parent vector $X_j^{(G)}$ using (5.14) instead of (4.15).

5.4.2 The outer loop iteration

After all PCs have finished the inner loop iteration, the master node starts the outer loop iteration by using the ALM method to handle the inequality constraints of the state variables. The details of the outer loop can be described as shown below.

1) Initialization

Set maximum iteration of the outer loop (N_o), the constrain violation tolerance (ε_{SVC}), the lagrange multiplier βs, and the penalty parameters r_g including c_g, and $r_{g,max}$.

2) Determined the best optimal inner loop iteration

The master node will determine the best optimal inner loop iteration ($X^*_{opt}{}^{(G\text{-}I)}$) by comparing the final result of all PCs based on the extent of the sum of the violated constraints (*SVC*) index in (5.25) and (5.26) and the total generator fuel cost in (5.6).

3) Verifying constrain violation

The constrain violation of the best optimal inner loop iteration (X^*_{opt}) is verified through the sum of the violated constraints (*SVC*) index as shown in (5.25) and (5.26).

4) Creating a new unconstrained minimization problem

A new unconstrained minimization problem through the new augmented lagrange function L_a is created by updating the lagrange multiplier βs and the penalty parameter r_g according to (5.23), and (5.24) respectively.

5) Appling the most feasible elitism

To improve the efficiency of the proposed algorithm, the most feasible elitism (X_{elite}) is employed by replacing the worst individual X_j which has the highest fitness value for the next inner loop iteration. The elitist member is initialized by using the optimal solution obtained from the first outer loop iteration. Then, it is updated according to the extent of the violated *SVC* value and the total generator fuel cost in (5.6) as described in section 4.4.2 of chapter 2. The outer loop will be terminated according to the same two criteria as defined for the inner loop, i.e. 1) maximum iteration number of the outer loop (N_o), and 2) convergence of the optimal solution.

5.5 Numerical Results

Both SADE_ALM and pSADE_ALM were implemented to solve the SCOPF problems based on the IEEE-30 bus system [65] given in Appendix D. The effectiveness of both algorithms has been tested and compared with other approaches, i.e. gradient based approach [65] and evolutionary programming (EP) [13] based on quadratic cost curve model as in case 4.1 of chapter 4. In addition, the SCOPF problems for the IEEE 57 and 118 bus system [66] were also implemented. The bus, generator, and branch data for the IEEE 57 and 118 bus system are presented in Appendix E and F respectively. The in-phase transformers for both test systems were

assumed to be adjustable tap setting in ranges of ± 10%. For each case, 10 independent runs were conducted. The parameters of SADE_ALM and pSADE_ALM for all test cases used the same setting as in section 4.5 of chapter 4. The programs were developed based on free numerical software SCILAB 4.0 [61] on PC Cluster 3x2.8 GHz Pentium IV processors with 256 MB RAM for each PC.

5.5.1 Case 5.1: The SCOPF with nine single-line outages for the IEEE 30 Bus System.

The SCOPF problems based on nine single-line outages (i.e., transmission lines numbered 1, 2, 4, 5, 7, 33, 35, 37, and 38) of the base-case OPF in case 4.1 of chapter 4 are considered in this case. The simulation results are shown in Table 5.1 and the convergence characteristic of pSADE_ALM and SADE_ALM is shown in Figure 5.3.

Table 5.1 Comparison of the total generator fuel costs for case 5.1

Algorithm	Fuel Cost ($/hr.)				Average computational time (minutes)
	Best cost	Average cost	Worst cost	S.D. of cost	
Gradient [65]	813.740	N/A	N/A	N/A	N/A
SADE_ALM	834.547	853.244	878.914	13.898	82.932
pSADE_ALM	826.978	826.978	826.978	0.000	157.401

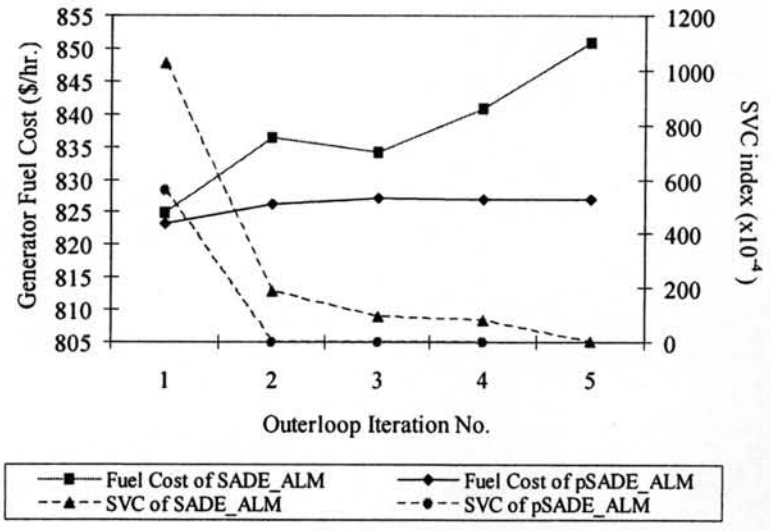

Figure 5.3 Convergence characteristic of pSADE_ALM and SADE_ALM in case 5.1

5.5.2 Case 5.2: The SCOPF with five single-line outages for the IEEE 30 Bus System.

As in case 5.1, the single-line outages of transmission lines numbered 1, 2, 3, 5, and 7 are considered as five contingency-case states. The simulation results are shown in Table 5.2 and the convergence characteristic of pSADE_ALM and SADE_ALM is shown in Figure 5.4.

Table 5.2 Comparison of the total generator fuel costs for case 5.2

Algorithm	Fuel Cost ($/hr.)				Average computational time (minutes)
	Best cost	Average cost	Worst cost	S.D. of cost	
EP [13]	813.730	N/A	N/A	N/A	N/A
SADE_ALM	826.979	829.495	832.009	1.905	46.896
pSADE_ALM	826.242	826.242	826.242	0.000	119.812

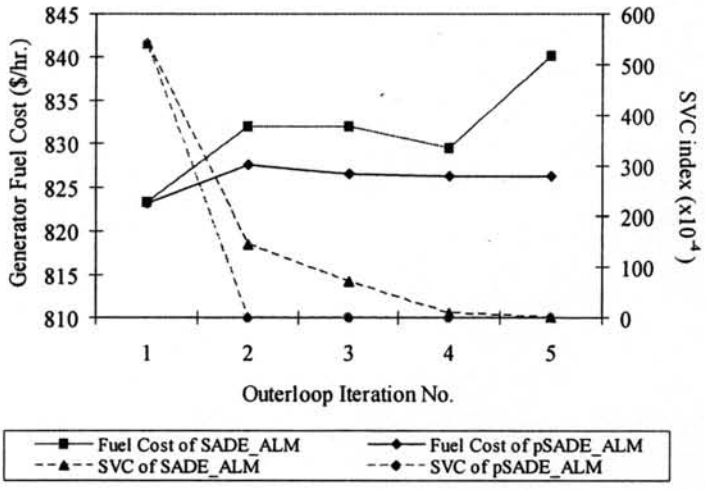

Figure 5.4 Convergence characteristic of pSADE_ALM and SADE_ALM in case 5.2

5.5.3 Case 5.3: The SCOPF for the IEEE 57 and 118 Bus System.

For this case, the SCOPF problems based on three single-line outages for the IEEE 57 bus system (i.e., transmission lines numbered 1, 3, and 7), and two single-line outages for the IEEE 118 bus system (i.e., transmission lines numbered 1, and 3) of the base-case OPF in case 4.5 of chapter 4 are considered in this case. The simulation results are shown in Table 5.3 and the convergence characteristic of pSADE_ALM and SADE_ALM for the IEEE 57 and 118 bus system are shown in Figure 5.5 and 5.6 respectively.

Table 5.3 Comparison of the total generator fuel costs for case 5.3

Test System	Algorithm	Fuel Cost ($/hr.)				Average computational time (minutes)
		Best cost	Average cost	Worst cost	S.D. of cost	
57 Bus	SADE_ALM	41914.318	43519.361	49513.808	2335.130	46.686
	pSADE_ALM	41724.443	41724.443	41724.443	0.000	180.496
118 Bus	SADE_ALM	145557.494	157279.294	186960.715	12630.824	59.963
	pSADE_ALM	132022.765	132022.765	132022.765	0.000	210.770

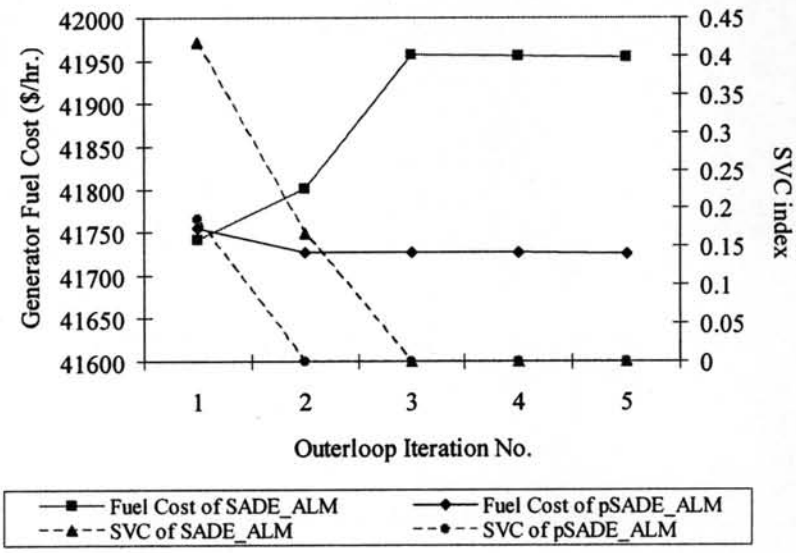

Figure 5.5 Convergence characteristic of SADE_ALM and pSADE_ALM for case 5.3 (the IEEE 57 bus system)

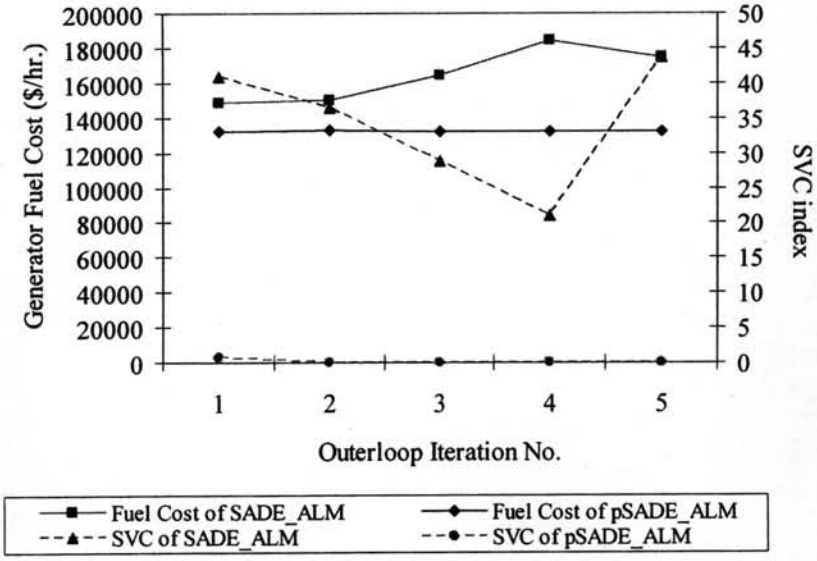

Figure 5.6 Convergence characteristic of SADE_ALM and pSADE_ALM for case 5.3 (the IEEE 118 bus system)

Based on the IEEE 30 bus system, numerical results in case 5.1 and 5.2 show that the best, the average, the worst and the S.D. of secure optimal solutions of pSADE_ALM are better than SADE_ALM as shown in Table 5.1 and 5.2 respectively. This reveals that the robustness of the secure optimal solutions determined from pSADE_ALM are better than SADE_ALM. Additionally, it has been found that the secure optimal solutions determined from both algorithms do not violate any constraints, whereas other approaches, i.e. conventional gradient method [65], and EP [13] violate line loading limit of their associated contingency constraints. For example, in case 1, the secure optimal solution reported by Alsac and Stott [65] violates line loading limit for four contingency cases, i.e. violates line loading limit of line 2 and 4 by +13.04% and 8.4 % respectively for outage of line 1, violates line loading limit of line 1 by +9.32% for outage of line 2, violates line loading limit of line 1 by +7.23% for outage of line 4, and violates line loading limit of line 6 and 8 by +3.74% and 9.97 % respectively for outage of line 5. In case 2.2, the secure optimal solution of EP reported by P. Somasundaram et.al. [13] also violates line loading limit for three contingency cases, i.e. violates line loading limit of line 2 and 4 by +13.08% and +8.30% for outage of line 1, violates line loading limit of line 1 by +9.45% for outage of line 2, and violates line loading limit of line 6 and 8 by +3.47% and +10.84% for outage of line 5.

The secure optimal values of the best solution given by both algorithms for case 5.1 and 5.2 are shown in Table 5.4. Tables G.1-G.4 in Appendix G show power flow results of SADE_ALM and pSADE_ALM based on the associated best secure optimal solution for case 5.1 and 5.2.

Using the same parameter setting, numerical results for case 5.3 reveal that pSADE_ALM also provide the best, the average, the worst, and the S.D. of secure optimal results better than SADE_ALM for higher system, i.e. the IEEE 57 and 118 bus systems as shown in Table 5.5. In addition, for all ten test runs, pSADE_ALM provides the same optimal solution for all trial runs without violating any constraints, whereas SADE_ALM violates constraints slightly in trial no. 2, 3, 4, 5, 7, 8, and 9 for 57 bus system, and all trials for 118 bus system as shown in Table 5.6.

The secure optimal values of the best solution given by SADE_ALM and pSADE_ALM for the IEEE 57 and 118 bus system are shown in Table H.1 and I.1 in Appendix H and I respectively. In addition, Tables H.2-H.3 and I.2-I.3 in Appendix H and I show power flow

results of SADE_ALM and pSADE_ALM based on the associated best secure optimal solution for 57 and 118 bus system respectively.

Table 5.4 The best secure optimal solutions given by SADE_ALM and pSADE_ALM in case 5.1 and 5.2

Optimal Solution	Secure optimum point (SCOPF) for the IEEE 30 Bus System			
	Case 1		Case 2	
	SADE_ ALM	pSADE_ ALM	SADE_ ALM	pSADE_ ALM
P_{G1} (MW)	122.4151	123.6109	123.4114	123.5861
P_{G2} (MW)	60.9828	61.9204	60.9517	62.0803
P_{G5} (MW)	33.0807	30.3969	28.6305	28.4438
P_{G8} (MW)	35.0000	34.7396	35.0000	35.0000
P_{G11} (MW)	25.7310	20.6554	21.4728	20.7483
P_{G13} (MW)	12.8100	18.2952	20.3961	19.9315
V_{G1} (p.u.)	1.0500	1.0500	1.0462	1.0500
V_{G2} (p.u.)	1.0357	1.0372	1.0349	1.0380
V_{G5} (p.u.)	0.9729	1.0051	0.9852	0.9967
V_{G8} (p.u.)	0.9871	1.0269	1.0169	1.0326
V_{G11} (p.u.)	1.1000	1.0925	1.0945	1.0979
V_{G13} (p.u.)	1.0374	1.0770	1.0452	1.0812
t_{11}	0.9916	1.0603	1.0887	1.0696
t_{12}	0.9000	0.9034	0.9482	0.9361
t_{15}	0.9252	0.9973	1.0051	1.0039
t_{36}	0.9296	0.9614	0.9574	0.9582
Fuel Costs ($/hr.)	834.547	826.978	826.979	826.242

Table 5.5 Secure optimal results for the IEEE 57 and 118 bus system given by SADE_ALM and pSADE_ALM for each trial run in case 5.3

Trial No.	IEEE 57 bus system				IEEE 118 bus system			
	SADE_ALM		pSADE_ALM		SADE_ALM		pSADE_ALM	
	Fuel Cost ($/hr.)	SVC index	Fuel Cost ($/hr.)	SVC index	Fuel Cost ($/hr.)	SVC index	Fuel Cost ($/hr.)	SVC index
1	41914.318	0.0000	41724.443	0	155970.067	10.8821	132022.765	0
2	49513.808	0.1875	41724.443	0	186960.715	9.7227	132022.765	0
3	42035.006	0.0022	41724.443	0	145557.494	5.9813	132022.765	0
4	43278.048	0.0563	41724.443	0	157516.065	5.4975	132022.765	0
5	43954.582	0.0311	41724.443	0	152323.295	17.1330	132022.765	0
6	42077.328	0.0000	41724.443	0	147645.613	21.3875	132022.765	0
7	44743.635	0.0120	41724.443	0	149256.653	18.2195	132022.765	0
8	43642.652	0.0159	41724.443	0	148295.650	11.2063	132022.765	0
9	42080.322	0.0609	41724.443	0	159886.623	11.5467	132022.765	0
10	41953.914	0.0000	41724.443	0	169380.761	4.5246	132022.765	0

5.6 Conclusion

The sequential self-adaptive differential evolution with augmented lagrange multiplier method (SADE_ALM) and parallel SADE_ALM called pSADE_ALM were applied to solve the SCOPF problems. The effectiveness of both algorithms has been tested based on the IEEE 30, 57, and 118 bus test system. Numerical results show that the pSADE_ALM is successfully and effectively implemented to find the global or quasi-global optimum for the SCOPF problems without violating any constraints compared with other approaches. In addition, the robustness of the optimal results determined from each trial for all test cases of pSADE_ALM is significantly better than SADE_ALM. However, the average computational time of pSADE_ALM for all test cases is higher than SADE_ALM. As in chapter 4, the main reason for this is that the computational time for inner loop iteration of pSADE_ALM are higher than SADE_ALM since the master node has to wait the elite members from every nodes including the master node before proceeding the outer loop iteration, whereas the SADE_ALM can proceed the outerloop iteration immediately without idle time. This drawback is still needed to be improved for future research.

In the next chapter, we will describe the mixed-integer SADE_ALM called MISADE_ALM. Since, in practical situation of the OPF problems, the optimal settings of control variables (e.g., shunt capacitors/reactors, and transformer tap-settings) are discrete in nature. The SADE_ALM may possibly provide the local optimal solutions after the continuous control variables are modified to the nearest discrete control variables. The details of the MISADE_ALM with numerical results are presented in the following chapter.